IEEE Robotics and Automation Letters (RA-L) paper, presented at ICRA 2026, Vienna, Austria. Cite as RA-L paper.

Development of Adaptive-Limb Transformable Robot for Portable and Replaceable End-Effectors With Compact Lock-Spin Mechanisms

Jin Hirai, *Student Member, IEEE*, Takuma Hiraoka, Masanori Konishi, *Graduate Student Member, IEEE*, Hiromi Tada, *Graduate Student Member, IEEE*, Kunio Kojima, and Kei Okada

***Abstract*—Transformable robots adapt to various environments by changing their shape or functionality. The robots are able to further expand their task range by replacing their end-effectors (EEs). In this letter, we propose an adaptive-limb transformable robot capable of replacing multiple types of mounted EEs. First, 7 degrees of freedom (DoF) limbs can reach multiple types of EEs mounted on the front body surface, and replace them using that single limb without relying on external devices. Second, we develop a compact Lock-Spin mechanism that integrates a locking mechanism into the rotor of the motor to enable continuous rotation. Experimental results demonstrate that the proposed transformable robot can replace EEs on-site and that this replacement enables locomotion and manipulation adapted to the environment.**

***Index Terms*—Legged robots, mechanism design, grippers and other end-effectors.**

I. Introduction

ROBOTS require different functionalities depending on the environment. Conventional mobile robots and manipulator arms are often limited in the range of tasks they can perform with their single configuration. In contrast, transformable robots adapt to diverse environments by changing their shape or functionality for different task modes. For example, in the DARPA Robotics Challenge [1], which aimed at practical operation in disaster environments, robots such as CHIMP [2], DRC-Hubo [3], [4], and RoboSimian [5] accomplished tasks by switching among task modes according to the environment. Thus, transformable robots are expected to enable flexible operation in harsh environments such as disaster sites and uneven terrain.

If transformable robots have the ability to replace end-effectors (EEs), they would further expand their task range. As shown in Fig. 1(a) and (b), the robot can walk using foot plates and manipulate using hooks. Specifically, adding continuous rotation capability to the EE expands its workspace and application range. As shown in Fig. 1(c) and (d), the robot can also handle tasks that require continuous rotation, such as wheeled locomotion and object lifting via wire-winding pulleys.

However, there are two requirements for the EE replacement with rotational functionality in transformable robots. First, in order to expand its task range, the robot must replace EEs in response to the local environment, which requires carrying them to allow on-site replacement. Second, a compact rotary locking mechanism is required to ensure secure coupling without compromising EE operability.

In this letter, we propose an adaptive-limb transformable robot that can carry and replace EEs, equipped with compact Lock-Spin mechanisms. The overview of the proposed adaptive-limb transformable robot is shown in Fig. 1. By using 7-DoF limbs capable of reaching the body, the robot replaces EEs between (I) the compact EE Lock-Spin mechanism on the distal limb to enable replaceability and (II) the EE gripper hand on the body to enable portability as shown in the left panel of Fig. 1. This allows the robot to switch among the diverse modes shown in the right panel of Fig. 1.

The main contributions of this letter are as follows.

i) We propose a novel configuration of a bipedal transformable robot with 7-DoF limbs capable of on-site EE replacement.
ii) We propose a method that utilizes the extended reach of the 7-DoF limbs to replace multiple types of EEs mounted on the body without relying on external devices.
iii) We design the EE Lock-Spin mechanism that transmits EE rotational torque through a compact locking structure while maintaining mechanical robustness.
iv) We show on the proposed robot that a single robotic platform can operate in both wheeled and walking locomotion modes, and can perform manipulation tasks using a hook and wire-winding pulleys.

This letter is organized as follows. Section II describes related works. Section III describes the body and limb structure of the adaptive-limb transformable robot developed in this letter. Section IV describes the detailed design of the EE Lock-Spin mechanism and EEs. Section V shows experimental results that demonstrate the robustness evaluation of the EE Lock-Spin mechanism, EE replacement by itself, and the motion experiments using multiple types of end-effectors. Section VI concludes this letter.

II. Related Work

Numerous studies on transformable robots have explored different strategies to extend their functional capabilities by altering

Received 14 July 2025; accepted 23 October 2025. Date of publication 19 November 2025; date of current version 1 December 2025. This article was recommended for publication by Associate Editor Y. Chitalia and Editor C. Della Santina upon evaluation of the reviewers' comments. *(Corresponding author: Jin Hirai.)*

The authors are with the Graduate School of Information Science and Technology, The University of Tokyo, Tokyo 113-8656, Japan (e-mail: hirai@jsk.imi.i.u-tokyo.ac.jp; t-hiraoka@jsk.imi.i.u-tokyo.ac.jp; konishi@jsk.imi.i.u-tokyo.ac.jp; h-tada@jsk.imi.i.u-tokyo.ac.jp; k-kojima@jsk.imi.i.u-tokyo.ac.jp; k-okada@jsk.imi.i.u-tokyo.ac.jp).

This article has supplementary downloadable material available at https://doi.org/10.1109/LRA.2025.3634910, provided by the authors.
Digital Object Identifier 10.1109/LRA.2025.3634910

IEEE Robotics and Automation Letters (RA-L) paper, presented at ICRA 2026, Vienna, Austria. Cite as RA-L paper.

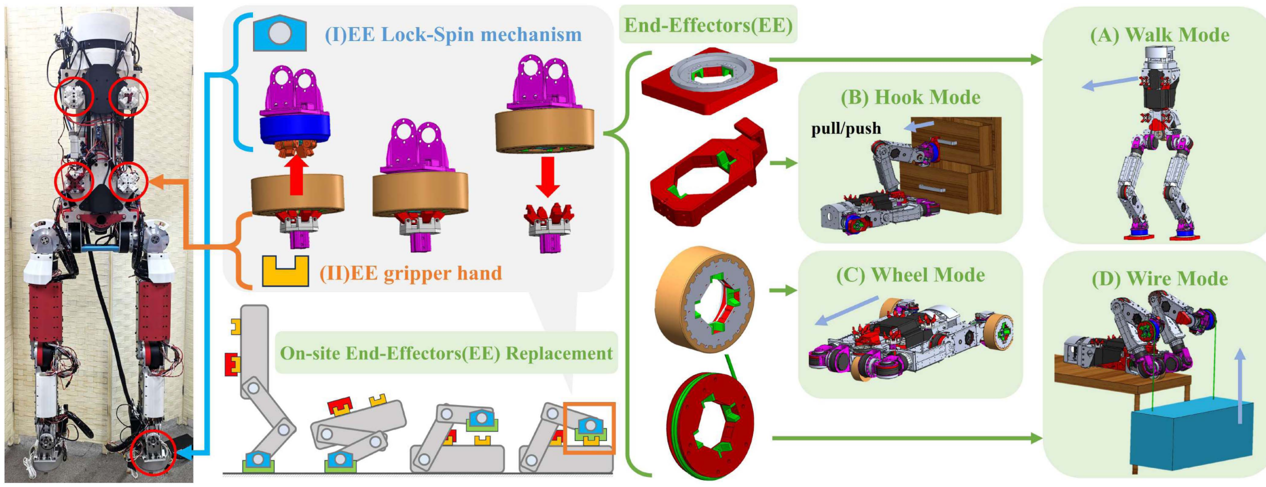

Fig. 1. Examples of the task range expansion in the adaptive-limb transformable robot through on-site End-Effectors (EEs) replacement between (I) the EE Lock-Spin mechanism located on the distal limb to enable replaceability, and (II) the EE gripper hand located on the body to enable portability: (A) Walking using foot plates, (B) Manipulation using hooks, (C) Locomotion using wheels, (D) Object handling using wire-winding pulleys.

how they interact with their environment. Additionally, some robots are equipped with detachable mechanisms for equipment or modules to further expand their task range. In this letter, we categorize related works into two groups: (A) methods for robots to act on the environment with EEs and (B) detachable mechanisms for equipment or modules.

A. Methods for Robots to Act on the Environment With EEs

We categorize three main approaches.

First, some robots use foot-end effectors to expand their task range [6], [7], [8]. The quadruped robot WAREC [6] achieves rough-terrain traversal and ladder climbing by manipulating foot-end effectors. ANYmal equipped with four non-steerable, torque-controlled wheels [7] and Go2-W [8] can switch between walking and wheeled locomotion in response to the environment. In all of these robots, the point of contact with the environment is limited to the feet.

Second, some robots switch their environmental contact points using dedicated embedded mechanisms [2], [3], [4], [9], [10]. CHIMP [2] is equipped with crawlers on both its arms and legs, which enables it to locomote via either set of crawlers depending on the terrain. DRC-HUBO [3], [4] switches between bipedal walking and locomotion with active wheels mounted at its knees. Lu et al. [9] developed a transformable robot that is able to switch between quadrupedal walking and wheeled motion using wheels attached at its waist. Shu et al. [10] developed a robot with crawlers mounted at two joints on each leg, which allows it to switch its ground-contact points in response to the terrain. In these robots, the mounting location of the environmental-interaction mechanism is tightly coupled with the DoF of the limbs, which limits the extensibility of their overall structure.

Third, some robots expand their task range through reconfiguration of EE structures [11], [12], [13], [14], [15], [16], [17]. TurboQuad [11], Modular Two-Degree-of-Freedom Transformable Wheels [12], and WheeLeR [13] each deploy claw-like treads or linkages to climb over obstacles. Quattroped [14] folds one side of its wheel to use it as a leg. A claw-wheel transformable robot [15] switches from claw mode to wheel mode by rotating its joints. Kimoto et al. [16] proposed a snake-like robot capable of transforming its segments into wheels by actuating its joints. Nakai et al. [17] developed a robot that changes shape through the phase change of low melting point alloy. In such robots, the EE structure and function are inherently integrated and inseparable.

B. Detachable Mechanisms for Equipment or Modules

We categorize two main approaches.

First, some passive methods for actuatorless EE replacement have been proposed [18], [19], [20]. ALDMag [18] uses a locking mechanism with springs and magnets, which enables changes to the joint structure of a small humanoid robot. Similarly, the actuator-free EE replacement mechanism [19] relies on a locking mechanism to change the structure itself. Pettinger et al. [20] developed a fully passive tool changer that uses only a compliant manipulator's contact forces. In such robots, external fixtures and environmental constraints are required during the replacement process.

Second, various active mechanisms using actuators for EE replacement have been proposed [21], [22], [23], [24], [25]. The genderless-docking mechanism [21] proposes a replacement system by electromagnets and springs in simulations. BEATLE, an aerial robot [22], can combine its parts using a switchable permanent magnet module and a stick insertion locking mechanism. M3Express [23] uses magnets and wedge by servo motors to enable transmission of rotational torque after docking. Industrial machines are examples of robots using tool changers [24], [25]. Despite their effectiveness, these actuator-based designs often tend to be mechanically complex and bulky. Consequently, integrating them into robotic EEs with limited space remains a significant challenge.

III. Design of Adaptive-Limb Transformable Robot With Portable and Replaceable EEs

The proposed transformable robot consists of two main components.

IEEE Robotics and Automation Letters (RA-L) paper, presented at ICRA 2026, Vienna, Austria. Cite as RA-L paper.

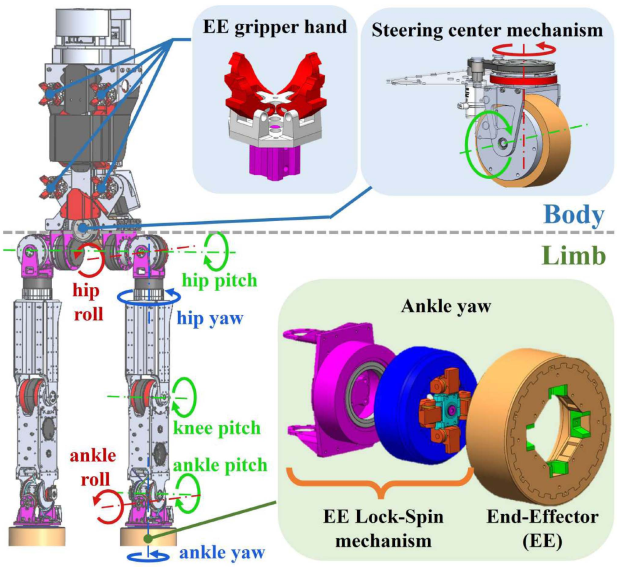

Fig. 2. The overall structure of the proposed transformable robot: The body equipped with multiple EE gripper hands and two 7-DoF limbs (hip pitch, hip roll, hip yaw, knee pitch, ankle pitch, ankle roll, and ankle yaw) with a wide range of motion.

TABLE I
PHYSICAL PARAMETERS OF THE ADAPTIVE-LIMB TRANSFORMABLE ROBOT

Items		Value
Mass	total	32.4 kg
	steering center mechanism	2.0 kg
	hip	4.2 kg
	knee	1.5 kg
	ankle	4.3 kg
	EE Lock-Spin mechanism (with EE)	1.5 kg
Range of Motion	hip pitch	-360 deg$\sim$360 deg[1]
	hip roll	-25 deg$\sim$100 deg
	hip yaw	-360 deg$\sim$360 deg[1]
	knee pitch	-162 deg$\sim$90 deg
	ankle pitch	-95 deg$\sim$60 deg
	ankle roll	-95 deg$\sim$60 deg
	EE Lock-Spin mechanism	continuous rotation
Distance between Joints	hip roll of different limbs	0.351 m
	hip roll - knee pitch	0.3865 m
	knee pitch - ankle pitch	0.2620 m
	ankle pitch - limb contact point	0.1492 m
Robot Size	robot height	1.45 m
	robot width	0.45 m

i) A body structure equipped with multiple EE gripper hands to carry multiple types of mounted EEs.
ii) A limb structure with 7-DoF and a wide range of motion to enable EE replacement.

Fig. 2 shows an overview of the body and limb structures. The main physical parameters of[1] the adaptive-limb transformable robot are listed in Table I.

A. Body Structure Equipped With Multiple EE Gripper Hands

To prevent self-collision during EE replacement, the EE gripper hand must protrude as little as possible from the robot body.

[1]While the hip pitch and yaw joints are mechanically capable of continuous rotation, cable-routing constraints limit the practical range to ± 360deg about the nominal pose.

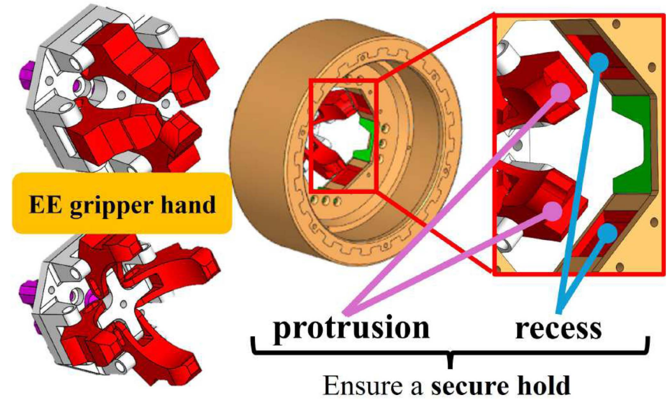

Fig. 3. The EE gripper hand has a compact structure with reduced thickness. Protrusions on the EE gripper hand and corresponding recesses on the EE enable a secure hold.

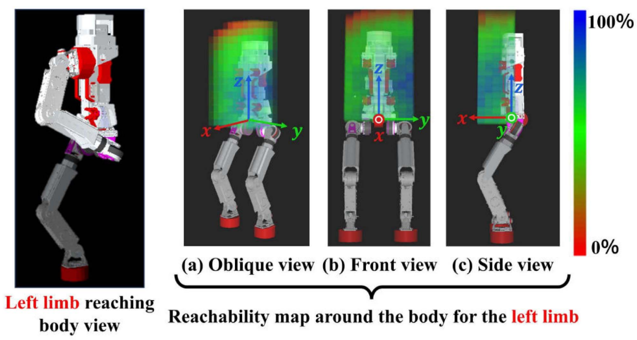

Fig. 4. The left panel shows the left limb EE reaching the body. The panel (a), (b), and (c) shows a reachability map around the body for the left limb EE. Evaluation with a position resolution of 50 mm to verify the possibility of replacement with the EE gripper hand.

By converting the linear motion of the air cylinder into rotation through a linkage mechanism, the design achieves a compact gripper hand with fewer components. Furthermore, as shown in Fig. 3, protrusions on the EE gripper hand and corresponding recesses on the EE enable a secure hold.

B. 7-DoF Limb Structure That Allows EE to Reach the Body

EE replaceability requires that the limb EE reliably reach the body. The limb shown in Fig. 2 is composed of 7-DoF with a wide range of motion: hip pitch, hip roll, hip yaw, knee pitch, ankle pitch, ankle roll, and ankle yaw (the EE Lock-Spin mechanism). We evaluate EE replaceability using a reachability map [26] with a spatial resolution of 50 mm over $[x, y, z]^\mathsf{T} \in [0, 200] \times [-200, 200] \times [0, 700]$, where all units are in mm. As shown in Fig. 4, the EE can access a broad region around the body, indicating sufficient reachability for the replacement.

IV. DESIGN OF COMPACT EE LOCK-SPIN MECHANISM

A. Design Concept

EE replacement mechanisms with continuous rotational functionality require a drive actuator. In addition, each limb of the robot requires an actuator that can exert continuous force to

IEEE Robotics and Automation Letters (RA-L) paper, presented at ICRA 2026, Vienna, Austria. Cite as RA-L paper.

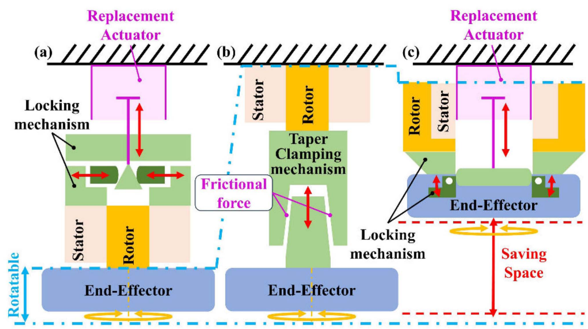

Fig. 5. Comparison of the placement of drive-force-required replacement mechanisms: (a) Conventional tool changer used in robotic arm, (b) Conventional tool changer used in machine tools, (c) Proposed EE Lock-Spin mechanism.

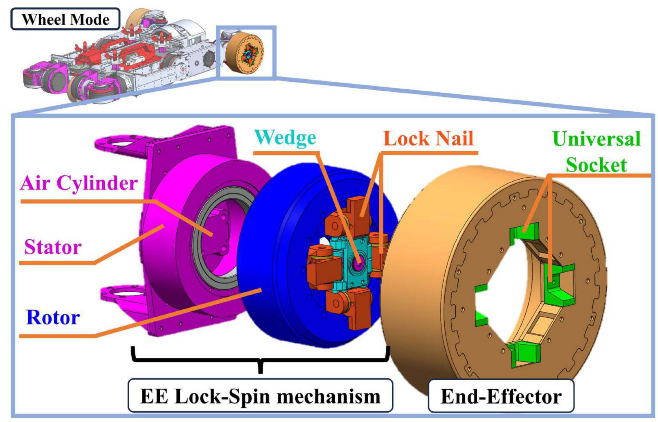

Fig. 6. Overview of the EE Lock-Spin mechanism. Integrating the air cylinder inside the motor enables a compact structure. The Wedge is the structure that actuates the Lock Nail.

replace EEs independently and on-site. Replacement EEs using two actuators must meet three design requirements.

i) Placement of the rotation drive actuator
ii) Post-replacement parts fixation and torque transmission
iii) Alignment of the rotation axis

i) The space of the mechanism is strongly influenced by where the rotation drive actuator is installed, so its placement must be optimized. ii) In order to transmit force to the EE after replacement, a robust locking mechanism and a torque transmission method are required. iii) Smooth operation demands that the rotational axis of the drive actuator and the EE be precisely aligned. Some replacement mechanisms that require driving force are broadly categorized into two types, as shown in Fig. 5.

The replacement structure shown in Fig. 5(a) illustrates the tool changer design used in robotic arms. As described by Little et al. [27], the locking mechanism used in robot tool changers features a low-profile structure. When a replacement actuator is used in conjunction with a drive actuator, the locking mechanism must be placed between them. Such an arrangement results in a completely serial stack. The overall axial length of the tool changer increases, and the EE which includes the drive actuator becomes larger.

The replacement structure shown in Fig. 5(b) illustrates the tool changer design used in machine tools. In the BT40 Holder [28], high-precision centering is achieved through a tapered spindle-tool interface, but the taper is not self-locking. Reliable fixation therefore depends on friction. In order to transmit enough torque, the system needs a broad friction surface and a pull-down force on the order of several kN; these requirements enlarge both the locking mechanism and the drawbar, which increase the tool changer's overall axial length.

Therefore, as illustrated in Fig. 5(c), we propose integrating the replacement actuator coaxially inside the drive motor. A taper-guided locking mechanism mounted at the tip of two actuators ensures precise centering of the EE. Furthermore, it achieves robust lock while transmitting rotational torque by allowing the locking mechanism to rotate.

In the remainder of this letter, we refer to this EE replacement mechanism as the EE Lock-Spin mechanism. An overview of the EE Lock-Spin mechanism is shown in Fig. 6, and its physical parameters are listed in Table II.

TABLE II
PHYSICAL PARAMETERS OF THE EE LOCK-SPIN MECHANISM

Items		Value
Total	Mass	1.05 kg
	Height (from the fixed surface)	58.2 mm
	Outside diameter	113.5 mm
Motor	Mass	0.71 kg
	Height	36.2 mm
	Hole diameter	74 mm
	Max torque	12 N m
Air Cylinder	Stroke length	15 mm
	Outside diameter	16 mm
	Force	140 N(at 0.7 MPa)

B. Detail Design of EE Lock-Spin Mechanism

The EE Lock-Spin mechanism is designed to meet the three design requirements outlined in Section IV-A.

1) Saving Space by Integrating Air Cylinder Into Motor: Integrating an air cylinder (replacement actuator) inside the motor (drive actuator) enables a compact structure. In order to achieve this, we selected a hollow outer-rotor motor (T-MOTOR RO100 KV55) with a separated stator and rotor. Table II shows that by embedding 34 mm of the air cylinder within the motor, the overall length is reduced to 58.2 mm. This configuration shortens the length by 36% compared with the assumed serial arrangement total length (34 mm + 58.2 mm = 92.2 mm). The EE Lock-Spin mechanism lacks a rotation shaft. An off-axis incremental encoder is therefore installed. The encoder and the motor's built-in Hall sensors enable position control with an angular resolution of 0.043deg (8192 counts per revolution).

2) Transmission of Rotational Torque by Lock Nail: The locking mechanism converts the linear motion of the air cylinder into rotational motion. Fig. 7 shows the locking and unlocking sequences.

The locking sequence is: (i) the air cylinder activates, and the Wedge pushes against the Lock Nail; (ii) the Lock Nail pivots under this force, and its 2deg taper angle of its surface ensures continuous engagement; (iii) the tapers of the EE Universal Socket of the EE and the EE Lock Nail engage with each other.

On the other hand, the unlocking sequence is: (i) the air cylinder retracts, which causes the Wedge to withdraw; (ii) the engagement of the Lock Nail is released; (iii) the EE becomes removable because the Lock Nail is released.

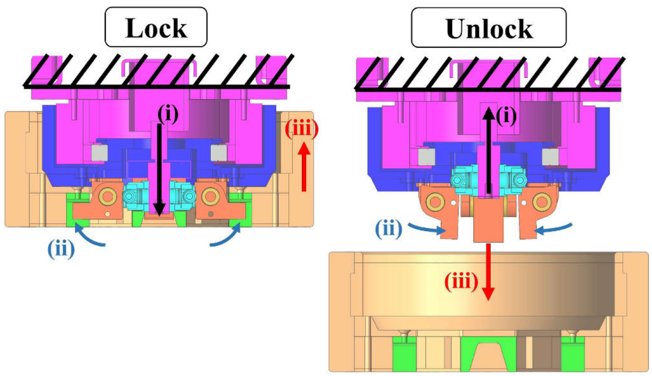

Fig. 7. Locking and unlocking actions of the EE Lock-Spin mechanism: (i) Action of the air cylinder (push / retract), (ii) Action of the Lock Nail (push / pull), (iii) Action of EE (fix / release).

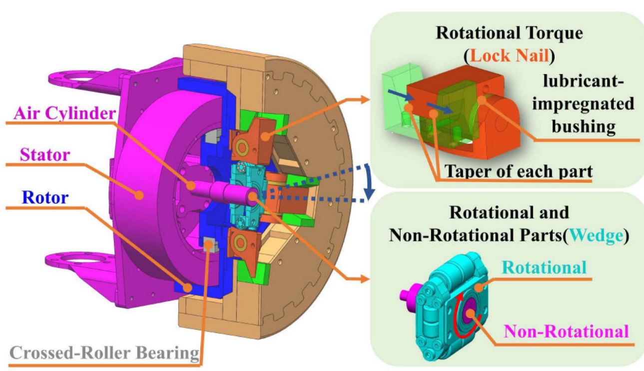

Fig. 8. Transmission of rotational torque in the EE Lock-Spin mechanism. The stator, and the air cylinder highlighted in the exterior view are rigidly attached to the limb, while the rotor, the Lock Nail, the Wedge, and the EE highlighted in the cross-sectional view are the rotating assembly. Rotational torque is transmitted by the Lock Nail.

To handle the axial loads imparted by the EE drive motor within limited clearance, we substitute a conventional thrust bearing with a lubricant-impregnated bushing at the Lock Nail.

3) Rotation by Wedge With Centering Capability: As shown in Fig. 8, the Wedge must also have a low-profile structure. The Wedge needs to transmit a stable force regardless of the contact position with the Lock Nail. Therefore, a mechanical element capable of rotational sliding is required and adopts a needle bearing which has high resistance to radial loads. By designing the Wedge to rotate around the axis of the air cylinder, the structure allows the Wedge to move in the vertical direction while preventing rotational force from being applied to the air cylinder axis. Additionally, precise centering can be achieved through taper-based alignment by utilizing the air cylinder axis as the center of rotation.

C. Detail Design of EEs Equipped With EE Universal Socket

As shown in Fig. 6, each EE is equipped with a common component - the EE Universal Socket. This common component allows the EE Lock-Spin mechanism and the EE gripper hand to be replaced with each other. Engagement of the matching taper surfaces on both components achieves a robust connection during the replacement.

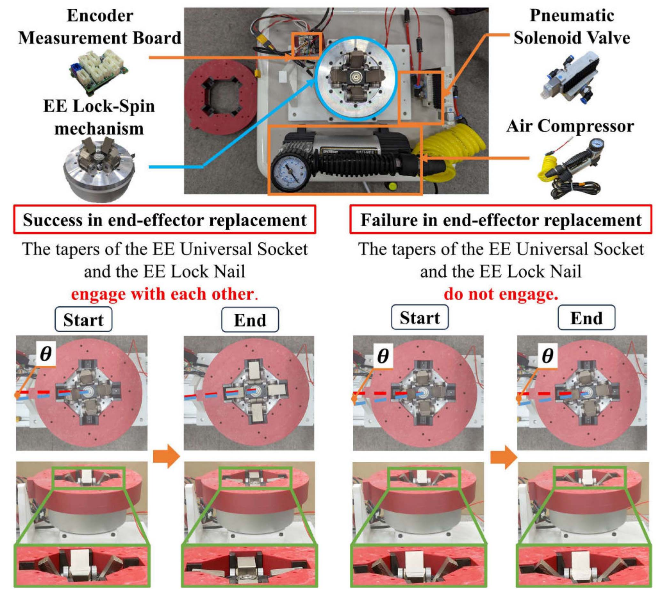

Fig. 9. Experimental setup for evaluating the rotational robustness of the EE Lock-Spin mechanism. Successful replacement means engagement between the EE Universal Socket and the EE Lock Nail. The angle θ denotes the angular difference between the EE and the EE Lock-Spin mechanism; red and blue dashed lines indicate their respective zero positions.

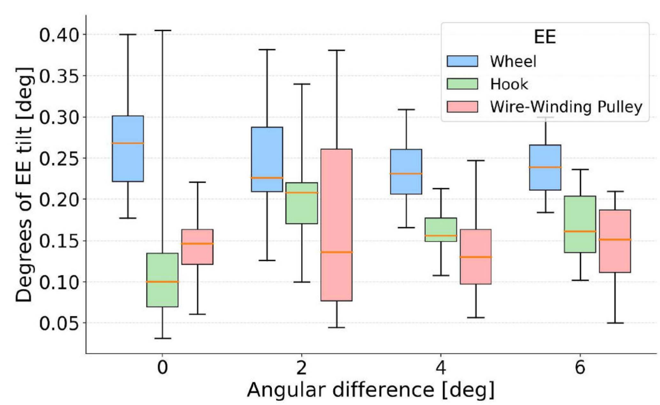

Fig. 10. Box-and-whisker plots of the EE (wheel, hook, wire-winding pulley) tilt when we conducted 15 trials at each angular difference. The maximum tilt after replacement was 0.405deg, so the absolute tilt values were stable. On the other hand, the wheel shows a slightly larger EE tilt (median) than the hook and the wire-winding pulley.

V. Experiment

In this section, we conduct experiments on the proposed adaptive-limb transformable robot to verify the following three aspects:

(A) To verify the robustness required for EE replacement, we evaluate the rotational robustness of the proposed EE Lock-Spin mechanism as shown in Section IV.

(B) To verify the effectiveness of the reachability evaluation presented in Section III, we perform experiments that the robot can replace multiple types of mounted EEs.

(C) To verify the robot's transformability, we demonstrate that the robot can achieve both locomotion and manipulation by using the replaced EEs.

IEEE Robotics and Automation Letters (RA-L) paper, presented at ICRA 2026, Vienna, Austria. Cite as RA-L paper.

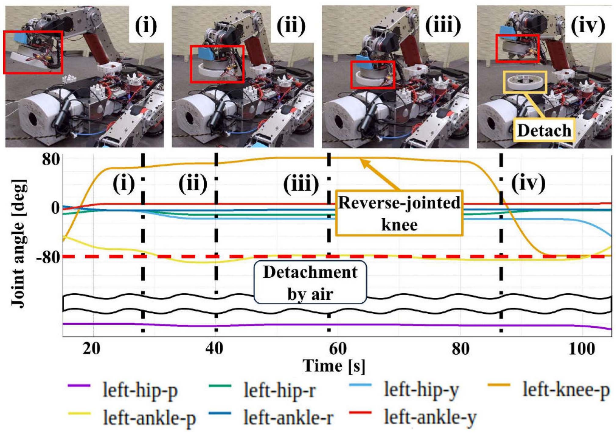

Fig. 11. Experiment on the EE detachment at the upper body EE gripper hand and logs of target angle. Grasp the EE with the upper body EE gripper hand and release the locking mechanism using the air cylinder with the EE Lock-Spin mechanism during (iii).

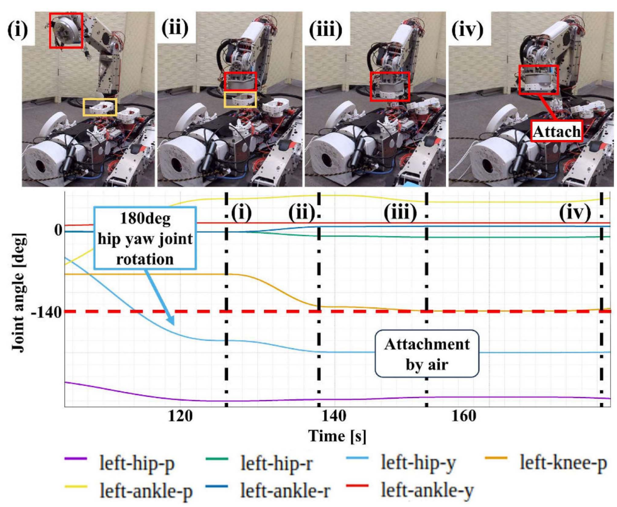

Fig. 12. Experiment on the EE attachment at the lower body EE gripper hand and logs of target angle. Fix the locking mechanism using the air cylinder with the EE Lock-Spin mechanism and release the EE with the lower body EE gripper hand during (iii).

A. *Robustness Evaluation of EE Lock-Spin Mechanism in the Rotational Direction*

The experimental setup for evaluating the robustness of the proposed mechanism in the rotational direction and examples of successful and failed replacement are shown in Fig. 9. After aligning the zero points of the EE and the motor, we offset the motor shaft in 2deg increments up to 8deg and conducted 15 trials at each angular difference, measuring the replacement success rate and the EE tilt after replacement. To examine differences across multiple types of EEs, we used a wheel (diameter 150 mm), a hook (top-view length 72 mm $\times$ width 145 mm), and a wire-winding pulley (diameter 120 mm). Replacement success or failure was determined by whether the tapers of the EE Universal Socket of the EE and the EE Lock Nail engage with each other. The angle θ denotes the angular difference between the EE and the EE Lock-Spin mechanism. The success rate in θ between the EE and the motor, and the EE tilt - denoting the residual angular errors between the rotational axis of the attached EE and that of the EE Lock-Spin mechanism - are shown in Table III and Fig. 10. For angular differences from 0deg to 6deg, all trials succeeded. The mean of the EE tilt after replacement did not exceed 0.271deg, and the maximum tilt was 0.405deg, so the absolute tilt values were stable. In contrast, for angular differences of 8deg or greater, all trials failed. These results indicate that the mechanism is sufficiently robust against angular differences up to 6deg. In order to increase capture tolerance to initial angular difference, the taper angle can be increased: however, a larger taper angle raises the pressing force required by the Lock Nail, thereby increasing the mechanical load. In future work, we will quantitatively establish design guidelines that balance capture tolerance and mechanical load by considering both the taper angle and the required pressing force.

TABLE III
ROBUSTNESS EXPERIMENT OF THE EE LOCK-SPIN MECHANISM: SUCCESS RATE IN THE ANGULAR DIFFERENCE (θ) BETWEEN EE (WHEEL, HOOK, WIRE-WINDING PULLEY) AND MOTOR, AND MEAN $\pm$ STANDARD DEVIATION (SD) OF THE EE TILT

EE	Angular difference (θ) (deg)	0	2	4	6	8
Wheel	Success rate	15/15	15/15	15/15	15/15	0/15
	Mean of EE tilt (deg)	0.271	0.242	0.233	0.242	\
	SD of EE tilt (deg)	0.0631	0.0697	0.0423	0.0347	\
Hook	Success rate	15/15	15/15	15/15	15/15	0/15
	Mean of EE tilt (deg)	0.137	0.199	0.159	0.166	\
	SD of EE tilt (deg)	0.105	0.0517	0.0274	0.0416	\
Wire-Winding Pulley	Success rate	15/15	15/15	15/15	15/15	0/15
	Mean of EE tilt (deg)	0.145	0.168	0.131	0.147	\
	SD of EE tilt (deg)	0.0391	0.106	0.0497	0.0467	\

The box-and-whisker plots in Fig. 10 also show that the wheel tends to exhibit a slightly larger median tilt after replacement than those of the hook and the wire-winding pulley. This is consistent with the geometry: the average distance from the center of the EE Lock-Spin mechanism to the EE's outer perimeter is larger for the wheel than the hook and the wire-winding pulley, so the outer edge lies farther from the Lock Nail-EE Universal Socket engagement point. An appropriate combination of EE geometry and taper angle enables a balanced design for the target task.

B. *Experiment on EE Replacement*

1) Experiment on EE Detachment Using the Upper Body EE Gripper Hand: Fig. 11 shows the experiment on the EE detachment at the upper body. The detailed steps for reaching a location far from the base joint are as follows.

i) Configure the knee joint as a reverse joint and adjust the ankle pitch to allow a 90deg bend to facilitate the subsequent inverse kinematics calculations.
ii) Move the EE + 60 mm in the vertical direction relative to the EE gripper hand. Rotate the EE Lock-Spin mechanism to an angle that allows detachment.
iii) Move the EE to the EE gripper hand. To ensure secure detachment, first grasp the EE with the EE gripper hand, then release the lock of the EE Lock-Spin mechanism.
iv) Extract it from the EE gripper hand by moving the EE to the same position as in step (ii).

2) Experiment on EE Attachment Using the Lower Body EE Gripper Hand: Fig. 12 shows the experiment on the EE

IEEE Robotics and Automation Letters (RA-L) paper, presented at ICRA 2026, Vienna, Austria. Cite as RA-L paper.

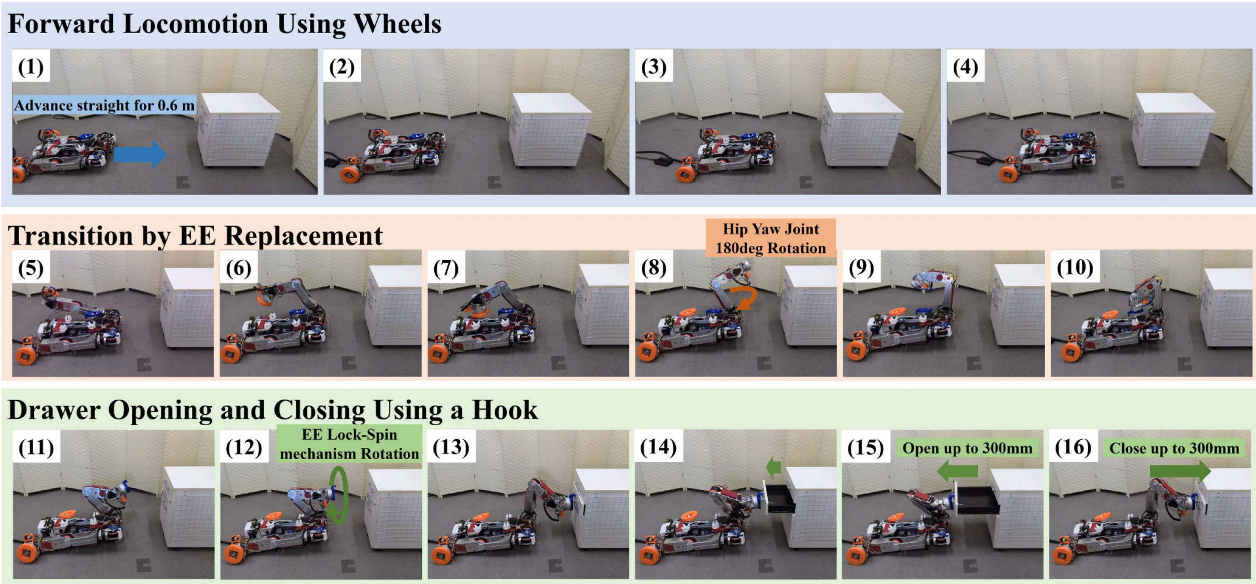

Fig. 13. Multi-mode experiments using wheels (orange EEs) and a hook (the blue EE). After 0.6 m of wheel-based locomotion, the proposed transformable robot replaced the EE on site. The robot opened and closed the drawer up to 300 mm using the hook.

attachment at the lower body. The detailed steps for reaching a location close to the base joint are as follows.

i) Command the hip yaw joint to -180deg from the angle used during replacement at the upper body and move the EE closer to the EE gripper hand.
ii) Move the EE + 60 mm in the vertical direction relative to the EE gripper hand. Rotate the EE Lock-Spin mechanism to an angle that allows attachment.
iii) Move the EE to the EE gripper hand. Engage the lock of the EE Lock-Spin mechanism, then release the grasp of the EE gripper hand to ensure secure attachment.
iv) Extract it from the EE gripper hand by moving the EE to the same position as in step (ii).

C. Experiments on Motion Using Multiple Types of EEs

1) Multi-Mode Experiments Using Wheels and Hook: As shown in Fig. 13, the proposed transformable robot performs multi-mode experiments using wheels and a hook.

Forward Motion Using Wheels: As shown in Fig. 2, the robot is supported at three contact points: one 107 mm-diameter wheel attached to the steering center joint, and two 150 mm-diameter wheels mounted on the EE Lock-Spin mechanism. Each wheel tracks its target under position control. The robot moves straight for 0.6 m.

EE Replacement: As also described in Section V-B, the EE is replaced between the EE Lock-Spin mechanism located on the distal limb and the EE gripper hands mounted on the upper and lower sections of the body. After detaching the wheel from the EE Lock-Spin mechanism, the robot rotates the hip yaw joint by 180deg while avoiding interference and then attaches the hook.

Drawer Opening and Closing Using a Hook: Manipulation is performed by hooking onto the environmental target. Using a hook 30 mm wide and 8.0 mm thick, we target an opening of 85 mm×19 mm located 420 mm above the ground. The EE Lock-Spin mechanism rotates to align the hook with the drawer front, after which the robot executes a pulling motion to open the drawer. The limb range of motion listed in Table I allows an opening and closing of up to 300 mm.

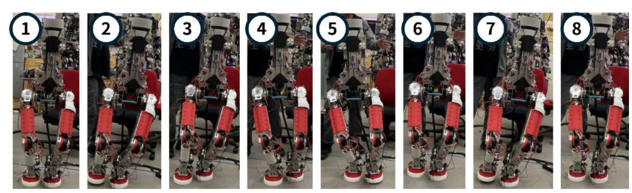

Fig. 14. Forward walking experiment. The robot moved forward by 0.21 m over 7 s.

2) Walking Motion Experiment Using Foot Plates: We conducted a forward walking experiment using foot plates, as shown in Fig. 14. We used a LIPM based gait controller [29]. The Zero Moment Point (ZMP) was continuously guided to remain near the center of the foot plates, and body posture was controlled through feedback from the IMU. The ankle joint was torque-controlled with low PD gains referred to the actuator input axis to absorb impact at landing and to follow sudden changes in ground reaction forces: $K_p = 20\,\text{Nm/rad}$ and $K_d = 0.3\,\text{Nms/rad}$. In contrast, the hip joint was position-controlled with high PD gains to preserve body stability: $K_p = 2800\,\text{Nm/rad}$ and $K_d = 200\,\text{Nms/rad}$. Both PD gains transitioned smoothly over time from step start to foot strike. As a result, the robot supported its own weight and walked; the robot moved forward by 0.21 m over 7 s. Higher walking speeds could be achieved with whole-body MPC or reinforcement learning.

3) Object Lifting Experiment Via Wire-Winding Pulleys: We conducted an object-lifting experiment via wire-winding pulleys. Fig. 15 shows the EE Lock-Spin mechanism rotated to reel in the wire that had been wound around the object and lifted the object. The robot started with a slack 5 mm-diameter wire, which was reeled in 120 mm-diameter pulleys, and successfully lifted a basket measuring 525 mm × 350 mm × 295 mm and weighing 1.95 kg by 250 mm.

IEEE Robotics and Automation Letters (RA-L) paper, presented at ICRA 2026, Vienna, Austria. Cite as RA-L paper.

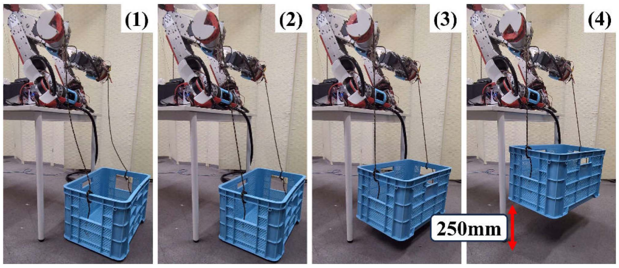

Fig. 15. Object lifting experiment using wire-winding pulleys. The robot successfully lifted a basket measuring 525 mm × 350 mm × 295 mm and weighing 1.95 kg by 250 mm using a 5 mm-diameter wire.

VI. Conclusion

Transformable robots are able to further expand their task range by replacing multiple types of EEs.

(a) This letter proposes a novel adaptive-limb transformable robot for portable and replaceable EEs with compact Lock-Spin mechanisms.

(b) Each limb of this robot has 7-DoF and a wide range of motion. Analysis of the reachability map confirms that the EE of the limb can reach the front surface of the body measuring 200 mm × 400 mm × 700 mm. The robot is able to vary its joint orientations for EE replacement at both the upper and lower body, which allows it to replace multiple types of EEs mounted on the body.

(c) We developed the EE Lock-Spin mechanism to transmit rotational torque through the locking mechanism, which saves space. This configuration shortens the length by 36% compared with the assumed serial arrangement total length. Evaluation experiments on the mechanism alone achieved a 100% success rate when the angular difference between the EE and the motor was kept within 6deg.

(d) We further demonstrated that the robot can switch between wheeled and bipedal locomotion, and perform manipulation tasks using a hook and a wire-winding pulley, simply by replacing its EEs.

In future work, we will integrate environmental perception so that the robot can select and replace EEs autonomously.

References

[1] E. Krotkov et al., "The DARPA Robotics Challenge Finals: Results and Perspectives," *J. Field Robot.*, vol. 34, no. 2, pp. 229–240, 2017.

[2] A. Stentz et al., "Chimp, the CMU highly intelligent mobile platform," *J. Field Robot.*, vol. 32, no. 2, pp. 209–228, 2015.

[3] T. Jung, J. Lim, H. Bae, K. K. Lee, H. -M. Joe, and J. -H. Oh, "Development of the humanoid disaster response platform DRC-HUBO," *IEEE Trans. Robot.*, vol. 34, no. 1, pp. 1–17, Feb. 2018.

[4] H. Bae, I. Lee, T. Jung, and J. -H. Oh, "Walking-wheeling dual mode strategy for humanoid robot, DRC-HUBO," in *Proc. 2016 IEEE/RSJ Int. Conf. Intell. Robots Syst.*, 2016, pp. 1342–1348.

[5] P. Hebert et al., "Mobile manipulation and mobility as manipulation—Design and algorithms of robosimian," *J. Field Robot.*, vol. 32, no. 2, pp. 255–274, 2015. [Online]. Available: https://onlinelibrary.wiley.com/doi/abs/10.1002/rob.21566

[6] K. Hashimoto et al., "Warec-1 — A four-limbed robot having high locomotion ability with versatility in locomotion styles," in *Proc. 2017 IEEE Int. Symp. Saf., Secur. Rescue Robot.*, 2017, pp. 172–178.

[7] V. S. Medeiros, E. Jelavic, M. Bjelonic, R. Siegwart, M. A. Meggiolaro, and M. Hutter, "Trajectory optimization for wheeled-legged quadrupedal robots driving in challenging terrain," *IEEE Robot. Automat. Lett.*, vol. 5, no. 3, pp. 4172–4179, Jul. 2020.

[8] "Go2-W (Unitree)," 2024. Accessed: Jun. 26, 2025. [Online]. Available: https://www.unitree.com/go2-w

[9] D. Lu et al., "Mechanical system and stable gait transformation of a leg-wheel hybrid transformable robot," in *Proc. 2013 IEEE/ASME Int. Conf. Adv. Intell. Mechatron.*, 2013, pp. 530–535.

[10] X. Shu et al., "A multi-configuration track-legged humanoid robot for dexterous manipulation and high mobility: Design and development," *IEEE Robot. Automat. Lett.*, vol. 8, no. 6, pp. 3342–3349, Jun. 2023.

[11] W.-H. Chen, H.-S.Lin, Y.-M. Lin, and P.-C. Lin, "Turboquad: A novel legwheel transformable robot with smooth and fast behavioral transitions," *IEEE Trans. Robot.*, vol. 33, no. 5, pp. 1025–1040, 2017.

[12] Y. Lee, S. Ryu, J. H. Won, S. Kim, H. S. Kim, and T. Seo, "Modular two-degree-of-freedom transformable wheels capable of overcoming obstacle," *IEEE Robot. Automat. Lett.*, vol. 7, no. 2, pp. 914–920, Apr. 2022.

[13] C. Zheng and K. Lee, "Wheeler: Wheel-leg reconfigurable mechanism with passive gears for mobile robot applications," in *Proc. 2019 Int. Conf. Robot. Automat.*, 2019, pp. 9292–9298.

[14] S.-C. Chen, K. -J. Huang, W. -H. Chen, S. -Y. Shen, C. -H. Li, and P. -C. Lin, "Quattroped: A leg–wheel transformable robot," *IEEE/ASME Trans. Mechatron.*, vol. 19, no. 2, pp. 730–742, Apr. 2014.

[15] J.-J. Chou and L.-S. Yang, "Innovative design of a claw-wheel transformable robot," in *Proc. 2013 IEEE Int. Conf. Robot. Automat.*, 2013, pp. 1337–1342.

[16] T. Kimoto, A. Yamano, M. Chiba, and T. Iwasa, "Modelling for rolling motion of snake-like robot using center of gravity shift," in *Proc. 2024 IEEE/SICE Int. Symp. Syst. Integration*, 2024, pp. 759–765.

[17] H. Nakai, Y. Kuniyoshi, M. Inaba, and H. Inoue, "Metamorphic robot made of low melting point alloy," in *Proc. IEEE/RSJ Int. Conf. Intell. Robots Syst.*, 2002, vol. 2, pp. 2025–2030.

[18] T. Makabe, K. Okada, and M. Inaba, "Development of the assembling system for structure transformable humanoid with attach-lock-detachable magnetic coupling," in *Proc. 2024 IEEE Int. Conf. Robot. Automat.*, 2024, pp. 2433–2439.

[19] J. Roux, J. -B. Izard, A. Tanguy, H. Kaminaga, F. Kanehiro, and A. Kheddar, "End-effectors changer design for humanoids," *IEEE Robot. Automat. Lett.*, vol. 9, no. 11, pp. 10495–10502, Nov. 2024.

[20] A. Pettinger, C. Dimoush, and M. Pryor, "Passive tool changer development for an elastic and compliant manipulator," in *Proc. 2019 IEEE 15th Int. Conf. Automat. Sci. Eng.*, 2019, pp. 1200–1205.

[21] J. Chen, X. Wen, H. Wang, W. Gong, Z. Deng, and H. Yu, "A genderless docking mechanism with passive locking and high rotation misalignment tolerance for modular space robots," in *Proc. 2022 IEEE Int. Conf. Robot. Biomimetics*, 2022, pp. 303–308.

[22] J. Sugihara, M. Zhao, T. Nishio, K. Okada, and M. Inaba, "Beatle—Self-reconfigurable aerial robot: Design, control and experimental validation," *IEEE/ASME Trans. Mechatron.*, vol. 30, no. 5, pp. 3537–3547, Oct. 2025.

[23] K. C. Wolfe, M. S. Moses, M. D. M. Kutzer, and G. S. Chirikjian, "M^{3}Express: A low-cost independently-mobile reconfigurable modular robot," in *Proc. 2012 IEEE Int. Conf. Robot. Automat.*, 2012, pp. 2704–2710.

[24] C. Obreja, G. Stan, D. Andrioaia, and M. Funaru, "Design of an automatic tool changer system for milling machining centers," *Appl. Mechan. Mater.*, vol. 371, pp. 69–73, 2013.

[25] M. I. Gökler and M. B. Koç, "Design of an automatic tool changer with disc magazine for a CNC horizontal machining center," *Int. J. Mach. Tools Manufacture*, vol. 37, no. 3, pp. 277–286, 1997.

[26] F. Zacharias, C. Borst, and G. Hirzinger, "Capturing robot workspace structure: Representing robot capabilities," in *Proc. 2007 IEEE/RSJ Int. Conf. Intell. Robots Syst.*, 2007, pp. 3229–3236.

[27] R. Little, "Tool changers enhance robot versatility," *Ind. Robot: An Int. J.*, vol. 30, pp. 306–309, Aug. 2003.

[28] W. W. Xiao, M. Zhu, K. M. Mao, and S. Lei, "Dynamic model of spindle-holder taper joint of BT40 holder," *Appl. Mechan. Mater.*, vol. 551, pp. 158–163, May 2014.

[29] Y. Kakiuchi et al., "Trajectory generation and compensation for external forces with a leg-wheeled robot designed for human passengers," in *Proc. 2022 IEEE-RAS 21st Int. Conf. Humanoid Robots (Humanoids)*, 2022, pp. 32–38.